Localization and Its Absence: A New Metallic State for Conducting Polymers

PHILIP PHILLIPS AND HONG-LU WU

A widely held view in solid-state physics is that disorder precludes the presence of long-range transport in one dimension. A series of models has been recently proposed that do not conform to this view. The primary model is the random dimer model, in which the site energies for pairs of lattice sites along a linear chain are assigned one of two values at random. This model has a set of conducting states that ultimately allow an initially localized particle to move through the lattice almost ballistically. This model is applicable to the insulator-metal transition in a wide class of conducting polymers, such as polyaniline and heavily doped polyacetylene. Calculations performed on polyaniline demonstrate explicitly that the conducting states of the random dimer model for polyaniline are coincident with recent calculations of the location of the Fermi level in the metallic regime. A random dimer analysis on polyparaphenylene also indicates the presence of a set of conducting states in the vicinity of the band edge. The implications of this model for the metallic state in other polymers, including heavily doped polyacetylene, are discussed.

E LECTRONIC STATES IN A CRYSTAL ARE ESSENTIALLY OF TWO types: they either carry current or they do not. Current-carrying states are spatially delocalized and extend over the entire crystal. States that do not carry current are confined or localized to a small region of the lattice. Typically, the envelope of a localized state decays exponentially from some lattice site in the crystal. When impurities are added to a crystal, the electronic states change fundamentally. Intuitively, one suspects that adding impurities would lead to scattering processes that would decrease the amplitude for the electron to move from one end of the crystal to the other. In 1958 the role that impurity scattering (disorder) plays in transforming delocalized electronic states into localized electronic states was revealed (1). Since then, Anderson's 1958 paper has stimulated a vast body of literature on insulator-metal transitions induced by disorder (1–15).

The model Anderson treated originally was the tight-binding approximation for the conduction band in a crystal, in which one orbital and a single random site energy are assigned to each lattice site. The site energies were chosen from a uniform distribution of width W. Let V be the electronic overlap connecting nearest

neighbor sites. Although the overall dynamics of this model depend in a complex way on the precise values of W and V, the transport properties in two simple limits can be identified immediately. When $W = 0$, an ordered system obtains because all of the site energies have the same value; transport is thus ballistic. For $V = 0$, none of the sites are connected and transport ceases. On physical grounds, then, one might suspect that gradually increasing the ratio of V/W in all cases would lead to a smooth interpolation between the limit of extreme localization ($V = 0$) and the ballistic regime (in which $V \gg W$).

We know now from Anderson (1) that this is not the case. The surprising result that Anderson showed [as did Mott and Twose (2) later] is that regardless of the strength of the nearest neighbor overlap V, all transport ceases in a one-dimensional (1-D) site-disordered lattice when $W > 0$. The absence of diffusion or long-range transport is generally viewed as the signature of the onset of exponential localization of the electronic eigenstates (1, 2). A more precise statement of Anderson's result, then, is that a lattice with site-diagonal disorder in one dimension possesses no eigenstates that have nonzero amplitudes on all the sites. That is, lifting the energetic degeneracy of the lattice sites even infinitesimally leads to exponential spatial decay of the eigenstates in one dimension. Although all proofs establishing quasi-particle localization in one dimension are model-dependent (2–6), exponential localization of all eigenstates in one dimension is viewed as a rigorous result. That is, quasi-particle localization in one dimension is considered to be unaffected by small details of the distribution of the site energies. In addition, short-range correlations are also thought to have little effect on the localization of the eigenstates of a 1-D disordered material (2–6). In their early work, however, Mott and Twose (2) expressed a modicum of caution regarding the universality of the 1-D result. They argued that "perhaps in all" 1-D systems, all states are localized (2, p. 107).

In this article, we review two disordered models we have recently proposed that exhibit surprising localization-delocalization transitions even in one dimension: (i) the random dimer model (RDM) (16) and (ii) its dual, the repulsive binary alloy (17). We show that in the RDM, if the site energies for pairs of lattice sites are assigned at random one of two values, a mobility edge separating conducting from insulating states will exist. The source of the delocalization is traced to a simple resonance effect. Special emphasis is given to the application of the RDM to conduction in the polymer polyaniline (18) and other similar conducting polymers, such as polypyrolle and polyparaphenylene. These polymers are similar in that (i) their ground states are nondegenerate and (ii) their conducting states are described by a disordered bipolaron lattice (19–22). We show in general that any disordered bipolaron lattice can be mapped onto a RDM. Our analysis shows that the RDM is of wide applicability to

The authors are in the Department of Chemistry, Massachusetts Institute of Technology, Cambridge, MA 02139.
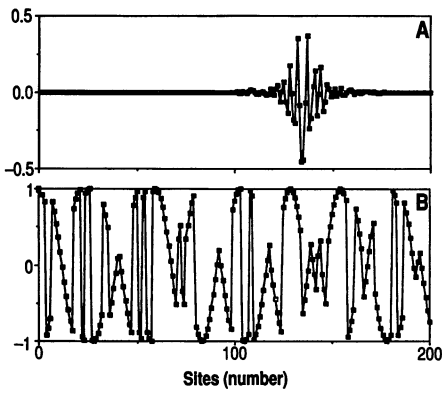
28 JUNE 1991

ARTICLES 1805

Fig. 1. (**A**) The real part of a typical eigenstate in a random binary alloy and (**B**) an unscattered eigenstate in the RDM. [(B) Reprinted from (16) with permission, © 1990 American Physical Society]

the insulator-metal transition in polymers that lack a degenerate ground state.

Random Dimer Model

To introduce the RDM, we focus on probably the simplest model exhibiting Anderson localization, the random binary alloy. In the tight-binding (or linear combination of atomic orbital) model of a random binary alloy, site energies ε_a and ε_b are assigned at random to the lattice sites with probability q and $1 - q$, respectively. When only site disorder is present, a constant nearest neighbor matrix element V mediates transport between the lattice sites. In one dimension, it is well accepted that for all nonzero q all the eigenstates will be exponentially localized, and no long-range transport will obtain at long times. A typical wavefunction in the random binary alloy is shown in Fig. 1A. The wavefunction does not spread over all the sites; it is localized. Consider a particular realization of the site energies in a certain segment of an infinite lattice: $\cdots\varepsilon_a\varepsilon_a\varepsilon_b\varepsilon_a\varepsilon_a\varepsilon_b\varepsilon_b\varepsilon_a\varepsilon_b\varepsilon_b\varepsilon_b\varepsilon_b\varepsilon_a\cdots$. Given the rigorous nature of the theorems establishing quasi-particle localization in one dimension, one can safely assume that the 1-D results are independent of both q and the number of ε_as or ε_bs that appear in clusters in the lattice. That is, the localization of 1-D quasi-particles still persists at zero temperature if all clusters containing an odd number of ε_bs are replaced by clusters containing an odd number of ε_as, for example. After all, under such a transformation the system is still random and the localization theorems guarantee an absence of transport for any degree of randomness in one dimension.

We have shown that this is not the case (16). In particular, we showed that when one of the site energies is assigned at random to pairs of lattice sites (that is, two sites in succession), $\sqrt{N}$ of the electronic states extend over the entire sample, where N represents the number of lattice sites. A delocalized eigenstate in the RDM is shown in Fig. 1B. We refer to a lattice in which at least one of the site energies is assigned at random to pairs of lattice sites as the RDM. An additional curiosity of the RDM is that the mean square displacement of an initially localized particle grows superdiffusively as $t^{3/2}$ (where t is time) provided that $-2V < \varepsilon_a - \varepsilon_b < 2V$. Diffusion obtains only when the disorder is increased such that $\varepsilon_a - \varepsilon_b = \pm 2V$. In all other cases, the particle remains localized at long times. Numerical simulations of the mean square displacement illustrating this behavior are shown in Fig. 2. Increasing disorder in the RDM smoothly interpolates between the limits of delocalization $|\varepsilon_a - \varepsilon_b| < 2V$ to the limit of extreme localization $|\varepsilon_a - \varepsilon_b| > 2V$. In contrast to the transport in the Anderson model, transport in the RDM is more in line with the physical intuition that increasing disorder should gradually (not abruptly) lead to an absence of transport. For this reason, the RDM is fundamentally different from

the standard site-disordered Anderson model, in which transport is at best diffusive only for $d > 2$, where d is the dimension of the lattice.

We can begin to understand the properties of the RDM by first focusing on an ordered lattice with a single dimer defect. We place the dimer on sites 0 and 1, assign the energy ε_a to all of the sites except sites 0 and 1, and let the energy of sites 0 and 1 be ε_b. A constant nearest neighbor matrix element V mediates transport between the sites. To calculate the scattering characteristics of a single dimer in this lattice, we compute the reflection and transmission coefficients through the dimer impurity. The eigenvalue equation for the site amplitudes C_n

$$EC_n = \varepsilon_n C_n + V(C_{n+1} + C_{n-1}) \tag{1}$$

where E represents energy, obeys the standard nearest neighbor Schrödinger equation. The site amplitudes are $C_n = e^{ikn} + Re^{-ikn}$ for $n \leq -1$ and $C_n = Te^{ikn}$ for $n \geq 1$ where R and T are the reflection and transmission amplitudes, respectively. From the eigenvalue equation for sites -1 and 1, it follows that $C_0 = 1 + R = T(\varepsilon_- e^{-ik} + V)/V$ with $\varepsilon_- = \varepsilon_a - \varepsilon_b$. Substitution of this result into the eigenvalue equation for site 0 results in the closed expression

$$|R|^2 = \frac{\varepsilon_-^2(\varepsilon_- + 2V\cos k)^2}{\varepsilon_-^2(\varepsilon_- + 2V\cos k)^2 + (2V^2\sin k)^2} \tag{2}$$

for the reflection probability. The reflection coefficient vanishes when $\varepsilon_a - \varepsilon_b = -2V\cos k$, which will occur for some value of k if $-2V \leq \varepsilon_a - \varepsilon_b \leq 2V$. The location in the parent-ordered band of the perfectly transmitted electronic state corresponds to the wave vector, k_0, where $|k_0| = \cos^{-1}[(\varepsilon_b - \varepsilon_a)/2V]$. At k_0 there is no difference between the ordered and disordered bands; the density of states coincides at this point. The vanishing of the reflection coefficient through a single dimer at a particular energy can be understood as a resonance effect. That is, the dimers are acting as resonance cavities. At a particular energy, the reflection from the second site in the dimer is 180° out of phase with the reflection from the first. At this energy, unit transmission obtains. The resonance is analogous to the transmission resonance that arises between two delta function potentials. The single cavity resonance is surprisingly preserved when dimers are randomly placed along a linear chain.

Of course, no transport would obtain if only a single electronic state remained unscattered. To determine the total number of states that extend over the entire sample, we expand R around k_0. To lowest order we find that in the vicinity of k_0, $|R|^2 \approx (\Delta k)^2$, where $\Delta k = k - k_0$. A crystal containing a certain fraction of randomly placed dimer impurities will have electronic states in the vicinity of k_0 reflected with a probability proportional to $(\Delta k)^2$. The time between scattering events τ is inversely proportional to the reflection probability. As a result, in the random system the mean free path $\lambda = (\text{velocity})\tau \approx 1/(\Delta k)^2$ in the vicinity of k_0. Let $\Delta k = \Delta N/2\pi N$. Upon equating the mean free path to the length of the system (N), we find that the total number (ΔN) of states whose mean free path is equal to the system size scales as $\Delta N\sqrt{N}$. Because the mean free path approximately equals the localization length in one dimension, total number of states whose localization lengths diverge is $\sqrt{N}$. Consequently, in the RDM $\sqrt{N}$ of the electronic states remain extended over the total length of the sample. Classical models such as the mass-disordered harmonic chain also have extended states but only at the band edge, $k = 0$ (6). The extended states in the RDM can occur anywhere in the band.

We can now estimate the contribution of the extended states to the transport properties. Because the mean free path of the extended states in the RDM is at least the system size, such states move

through the crystal ballistically with a constant group velocity [$v(k)$], except when they are located at the bottom or the top of the band, where the velocity vanishes. Because all of the other electronic states are localized, the diffusion constant is determined by integrating $v(k)\lambda(k)$ over the width of k-states that participate in the transport. The upper limit of the integration is then proportional to the total fraction of unscattered states or $1/\sqrt{N}$ and $\lambda(k) \approx N$. When the velocity is a nonzero constant, we obtain that the diffusion coefficient $D \approx \sqrt{N}$. Because the states that contribute to transport traverse the length of the system with a constant velocity, t and N can be interchanged or $D \approx t^{1/2}$. Consequently, the mean square displacement grows as $t^{3/2}$. At the bottom or the top of the band, where the group velocity vanishes, $v(k) \approx k$ and $D \approx 0$ (1). The formal definition of the mean square displacement is

$$\overline{m^2} = \sum_m m^2 |C_m|^2 \qquad (3)$$

where C_m is the site amplitude defined in Eq. 1. Numerical simulations that confirm the time dependence of the mean square displacement presented here are shown in Fig. 2. In addition, the conductance $|T|^2/|R|^2$ diverges at the energy at which $|R|^2 = 0$. This behavior is in contrast to the off-diagonal disorder problem, which has a vanishing conductance even at the band center ($E = 0$) where the localization length diverges (12). This behavior can be attributed to the fact that the reflection coefficient in this model does not vanish at $E = 0$ as it does in the RDM.

We now construct explicitly the unscattered states in the RDM. In the absence of any dimer impurities, the eigenstates are simply Bloch states of the form e^{ikn}. When the dimer impurities are present, because the eigenstates in the vicinity of k_0 have unit transmission, these states are still of the Bloch form. These states can be constructed as follows. Consider the single dimer impurity case discussed earlier. The dimer impurity is located on sites 0 and 1. The unscattered state must be of the form e^{ikn} for $n \leq 0$ and $e^{i(kn + \Omega)}$ for $n \geq 1$. That is, the only difference between the electron wavefunction before and after it has interacted with the impurity is that its phase changes by Ω. There is no reflected component. To determine Ω, we consider the eigenvalue equation $E - \varepsilon_b = V(e^{ik + \Omega} + e^{-ik})$ for site 0. This equation has a trivial solution with $\varepsilon_a = \varepsilon_b$ or equivalently in the limit of an ordered system. In this case $\Omega = 0$. The nontrivial solution occurs when $E - \varepsilon_b = 0$. Recall that when $E - \varepsilon_b = 0$, the reflection coefficient vanishes and the product of two b-type transfer matrices yields the unit matrix. Because E is the energy of the ordered band $\varepsilon_a + 2V\cos k$, the vanishing of $E - \varepsilon_b = 0$ corresponds to the condition $-2V \leq \varepsilon_a - \varepsilon_b \leq 2V$. In this case, $\Omega = -2k + \pi$. Consequently, the Bloch state that satisfies the Schrödinger equation is e^{ikn} for $n \leq 0$ and $-e^{ik(n-2)}$ for $n \geq 1$, provided that $-2V \leq \varepsilon_a - \varepsilon_b \leq 2V$. The wavefunction on the second atom of the dimer is the negative of the a-type atom located on site -1. If another dimer were located on sites 2 and 3, the corresponding perfectly transmitted wave would be $\cdots e^{-2ik}, e^{-ik}, 1,$ $-e^{-ik}, 1, e^{-ik}, 1, e^{ik}, e^{2ik}, \cdots$, provided of course that $-2V \leq \varepsilon_a - \varepsilon_b \leq 2V$. Such states can be constructed regardless of the number of dimer impurities that are placed at random in the lattice. Figure 1B shows the real part of a perfectly transmitted electronic state at a particular value of k for a dimer concentration of 50%. The electronic state is extended, although "scattering" occurs at each dimer.

The delocalization characteristics of the RDM are completely compatible with the standard localization theorems. A standard test of the onset of localization is the vanishing of the imaginary part of the self-energy [ImS(E)] along the real energy axis (3). The inverse of ImS(E) determines the lifetime of the state at energy E. Consequently, if ImS(E) vanishes, the state at energy E is a localized state.
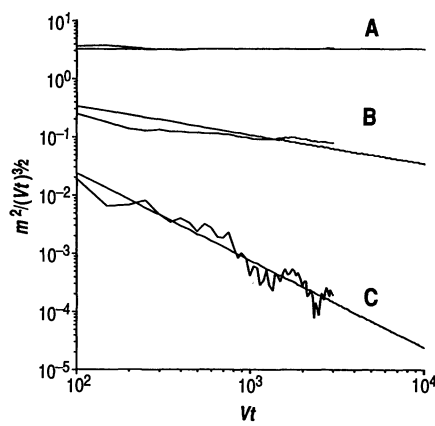

Fig. 2. The mean square displacement divided by $(Vt)^{3/2}$ for varying amounts of disorder in the RDM: Curve A, $\varepsilon_a - \varepsilon_b = V$, curve B, $\varepsilon_a - \varepsilon_b = 2V$, and curve C, $\varepsilon_a - \varepsilon_b = 3V$. The mean square displacement grows as $t^{3/2}$ in A, linearly as t in B, and is bounded for C. [Reprinted from (16) with permission, © 1990 American Physical Society]

One can easily verify that ImS(E) vanishes at all energies for the RDM. This is probably the reason the RDM was not discovered until recently. The vanishing of ImS(E) for the RDM can be understood as follows. The value of ImS(E) is determined by the nature of the singularities of the Green function. In fact, ImS(E) will only be nonzero if the Green function has an imaginary part or equivalently has a branch point singularity. The presence of a branch point signifies the presence of overlapping states. Isolated singularities or simple poles indicate the presence of localized states. An infinitesimal number of extended states is not sufficient in the thermodynamic limit to give rise to a branch cut of nonvanishing width. Consequently, ImS(E) will vanish for all energies in the RDM. As a result, the standard localization theorems (1–3) are completely consistent with the occurrence of a set of delocalized states of zero measure. Surprisingly, they are of sufficient number $\sqrt{N}$ to give rise to transport. As mentioned above, the extended state in the off-diagonal disorder problems, in direct contrast to the extended states in the RDM, is insufficient to give rise to a nonzero conductance. Pendry (8) has shown that in standard disordered models, isolated states at particular energies remain extended over $\sqrt{N}$ of the lattice sites. However, the number of states that behave in this fashion is exponentially small (8). As a result, such states, in contrast to the extended states in the RDM, do not affect the asymptotic value of the mean square displacement of an initially localized particle.

Conducting Polymers: The Metallic State in Polyaniline

In this section, we illustrate how the RDM is applicable to the insulator-metal transition in the conducting polymer polyaniline. In contrast to metals, polymers are typically insulators. Many industrial applications of polymers are based on their inability to carry current. However, in recent years new classes of polymers have been synthesized that are capable of carrying unusually high currents. For example, in 1977 a doped form of polyacetylene was reported to have a conductivity on the order of 10^3 S/cm (23). Because interchanging the double and single bonds in polyacetylene results in an equivalent structure, the ground state of this polymer is termed degenerate. The transport properties of this polymer are intrinsically tied to this degeneracy. Su, Schrieffer, and Heeger (24) suggested that soliton-like excitations from either ground state are responsible for the observed insulator-metal transition in polyacetylene. In recent years a new class of conducting polymers has been discovered experimentally that is different in kind from polyacetylene. Polymers such as polyaniline, polypyrrole, and polythiophene all lack a degenerate ground state but have high conductivities when doped
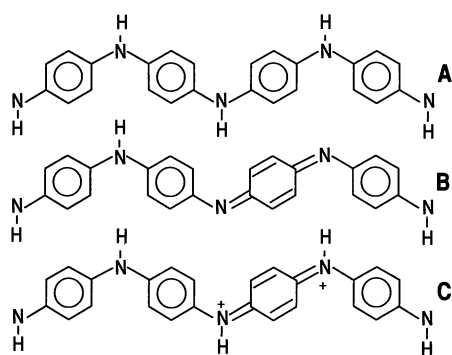
Fig. 3. Parent forms of polyaniline: (**A**) leucoemeraldine, (**B**) emeraldine, and (**C**) protonated emeraldine in the bipolaron model. [Reprinted from (*36*) with permission, © 1991 American Physical Society]

appropriately (*18, 25–27*). Consequently, one must invoke a mechanism distinct from the soliton conduction in polyacetylene to explain the high conductivities in this class of quasi-1-D conductors.

To illustrate the connection between the RDM and the polyaniline class of conducting polymers, we will explicitly perform the mapping of polyaniline onto the RDM. We choose polyaniline as our paradigm system because of the extensive experimental and theoretical data available. Let us start by summarizing the experimental work. Polyaniline refers to the general class of aromatic rings of benzenoid and quinoid character connected by nitrogen. The parent form of the polymer containing only benzenoid rings is referred to as leucoemeraldine. Emeraldine, on the other hand, contains a mixture of benzenoid and quinoid rings. These parent forms of the polymer are shown in Fig. 3, A and B. Both parent forms of polyaniline are insulators. However, upon electrochemical oxidation of the leucoemeraldine or acidification of the emeraldine parent, polyaniline undergoes an insulator-metal transition (*18, 28*). Experimentally, the metallic phase is characterized by a conductivity on the order of 10 S/cm, a value 10^{11} times the conductivity in the insulating forms of the polymer (*18, 28*).

The dramatic increase in the conductivity upon oxidation or acidification has sparked recent experimental work on polyaniline (*18–23, 28, 29*). Theoretical interpretations (*19, 30–34*) of the insulator-metal transition in polyaniline have been shaped by the observation that the Pauli susceptibility appears to be proportional to the degree of protonation or oxidation of the polymer (*22*). Physically, this behavior signifies that on the metallic side, the material is inherently inhomogeneous and phase-segregates into oxidized or protonated metallic islands embedded in a sea of insulating islands. Consequently, the view that polyaniline is a granular polymeric metal has emerged (*28*). However, not all experimental findings support this view (*29*). For example, the momentum dependence of the energy loss spectrum of the electron does not corroborate the granular metal picture (*29*). Recent calculations (*33*) suggest that the grain size required by the granular metal picture is at the least inconsistent with the experimental data on polyaniline derivatives.

Regardless of which global picture of polyaniline is most appropriate, the finding that polyaniline on the metallic side has conducting domains with high spin concentration appears to be intact. For example, recent electron spin resonance (ESR) and nuclear magnetic resonance (NMR) experiments by Mizoguchi *et al.* (*22*) have provided clear evidence for the conducting domain picture. The most surprising result of this experiment, however, is that the conducting domains do not correspond to three-dimensional (3-D) islands, as in the granular metal picture, but rather to single strands or few strands of the polymer (*22*). In polyaniline, single strands of the polymer contain 1000 or more repeat units (*35*). However, in a given sample the length of single strands can vary depending on the

sample preparation. Mizoguchi *et al.* (*22*) concluded as did Glarum and Marshall (*21*) that polyaniline is a unique example of a 1-D conductor in which the conductivity is carried by single strands of the polymer. These results are particularly important in light of recent extensive molecular orbital calculations by Galvao *et al.* (*19*) on single strands of randomly protonated emeraldine. Galvao *et al.* performed a series of calculations on linear chains of the polymer containing at least 200 rings of benzenoid or quinoid character (*19*). The quinoid rings were randomly placed in an otherwise ordered chain of benzene rings connected by nitrogen. Galvao *et al.* concluded that (i) the peak in the absorption spectrum at 1.5 eV is intrinsically tied to disorder and that (ii) upon protonation of the emeraldine form of the polymer, the Fermi level moves within the band to a region where extended states are located (*19*). They concluded, then, that the insulator-metal transition in polyaniline arises from the movement of the Fermi level (upon protonation or oxidation) to conducting states located in the vicinity of the band edge. The precise origin of the extended states in the calculations of Galvao *et al.* (*19*) is somewhat of a puzzle because they considered a disordered 1-D chain. As we have discussed above, all the electronic states in a disordered 1-D lattice should be exponentially localized.

If the insulator-metal transition in polyaniline is in fact tied to the presence of such states, it is crucial that the origin of such states be explained. We have recently shown that the extended states in a randomly protonated chain of emeraldine of arbitrary length can be explained by the RDM (*36*). We review this calculation here. The starting point for our analysis is the single strand of the emeraldine polymer shown in Fig. 3B. In the calculations of Galvao *et al.* (*19*), quinoid rings were randomly placed in an otherwise ordered chain of benzene rings connected by nitrogen. In the protonated form (*19*) of the polymer, the double-bonded nitrogens on either side of a quinoid ring were protonated as illustrated in Fig. 3C. Optical absorption data (*19*) and ESR data of Glarum and Marshall (*21*) strongly suggest that the protonated form of emeraldine constitutes a bipolaron lattice. In fact, the close agreement of the work of Galvao *et al.* (*19*) with the experimental data is further evidence that the disordered bipolaron lattice is stable and sufficient to describe the conducting form of the polymer. This agreement is clear evidence that the conducting state in polyaniline is populated by bipolarons. Because the present analysis does not include electron-electron interactions, a definitive answer cannot be given in regard to the spin of the charge carriers. The noninteracting picture we adopt is one in which a quasi-particle moves in a background of paired defects (bipolarons).

There seems to be some debate in the literature (*37*) as to whether the bipolaron lattice is disordered. On physical grounds, it is clear that if leucoemeraldine is oxidized 20%, one-fifth of the nitrogens will be positively charged. The occurrence of these charges in single strands of the polymer will be random if the counterions are present. Experimental evidence suggests that even at 50% oxidation, the bipolarons in emeraldine are still disordered (*19*). Researchers have made heuristic attempts based on an ordered bipolaron band to explain the conductivity in the polyaniline family of conducting polymers (*26*). The standard view is that at low doping levels, the Fermi level lies in the band gap. As the doping level increases, the upper and lower bipolaron bands broaden and eventually merge as the conductivity nears its maximum. This simple picture is not at all applicable when disorder is present, however, because the band structure is fundamentally different (*19*). For example, we know from Anderson (*1*) that the states in the bipolaron bands should be localized states that carry no current when disorder is present. We want to show that the disordered bipolaron model for the protonated form of emeraldine is a subset of the RDM and naturally has a set of conducting states coincident with the Fermi level.

To proceed, we consider the standard nearest neighbor, π-electron, tight-binding model for the quinoid defect shown in Fig. 4A for a typical strand of emeraldine. The atoms in the polymer chain are grouped into cells indexed by the label n (Fig. 4A). The label n indicates the nth nitrogen. The second label, ranging from one through six, indicates each carbon in the quinoid or benzene ring. We want to show that the eigenvalue equation $(E - \varepsilon_1)C_n = t_2 C_{n,1} + t_2 C_{n-1,2}$ for the nth nitrogen can be re-written entirely in terms of the nitrogen site amplitudes C_{n-1} and C_{n+1}. The matrix element t_2 (or t_2') transfers an electron from a nitrogen double-bonded (or single-bonded) to a carbon, ε_1 is the site energy for the π-electrons on nitrogen, and t_0 (or t_1) is the matrix element between two double-bonded (or single-bonded) carbon atoms. Hence, we will have effectively integrated out the quinoid (or the benzene) ring. What will be left will be the RDM. The eigenvalue equation for each atom obeys an equation analogous to Eq. 1. To proceed, we sum the eigenvalue equations for sites $n,3$ and $n,4$ and for sites $n,5$ and $n,6$. From the two simultaneous equations, we obtain that

$$C_{n,3} + C_{n,4} = T_1 C_{n,1} + T_2 C_{n,2} \tag{4}$$

and

$$C_{n,5} + C_{n,6} = T_1 C_{n,2} + T_2 C_{n,1} \tag{5}$$

with $T_1 = 2Et_1/(E^2 - t_0^2)$ and $T_2 = 2t_0 t_1/(E^2 - t_0^2)$. We now substitute these results into the eigenvalue equations for sites $n,1$ and $n,2$. Similarly, from the simultaneous equations, we obtain that $C_{n,1} = \widetilde{V}_1 C_n + \widetilde{V}_2 C_{n+1}$ and $C_{n,2} = \widetilde{V}_2 C_n + \widetilde{V}_1 C_{n+1}$, with

$$\widetilde{V}_1 = t_2(E - t_1 T_1)/[(E - t_1 T_1)^2 - (t_1 T_2)^2] \tag{6}$$

and

$$\widetilde{V}_2 = t_2 t_1 T_2/[(E - t_1 T_1)^2 - (t_1 T_2)^2] \tag{7}$$

If we now substitute these results into the eigenvalue equation for site n, we obtain the expression

$$(E - E_1)C_n = V_1 C_{n+1} + V_0 C_{n-1} \tag{8}$$

which involves only the nitrogen site amplitudes. In this expression, $V_1 = t_2 \widetilde{V}_2$ and $V_0 = t_2' \widetilde{V}_2'$, where the prime on $\widetilde{V}_2'$, where the prime on $\widetilde{V}_2'$ indicates that t_2 has been replaced with t_2'. The new site energy for a nitrogen associated with a quinoid defect is $E_1 = \varepsilon_1 + t_2 \widetilde{V}_1 + t_2' \widetilde{V}_1$. The new lattice contains the same information as first, except that effective matrix elements V_1 and V_0 have been derived that connect nearest neighbor nitrogens. In the new lattice, when a quinoid defect is present, nearest neighbor nitrogens
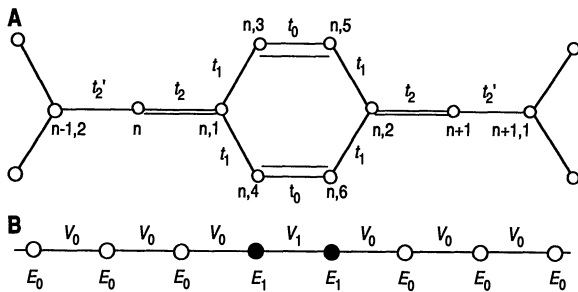
Fig. 4. (A) A typical quinoid defect in emeraldine. The label n denotes the nitrogen atoms, and the numbers from one to six label the carbons on the quinoid ring. The nearest neighbor transfer matrix elements are indicated by t_1, t_0, t_2, and t_2'. **(B)** The reduced RDM of emeraldine. The effective matrix elements (V_1 and V_0) arise and site energies (E_0 and E_1) arise from integrating out the benzene and quinoid rings. [Reprinted from (36) with permission, © 1991 American Physical Society]

Fig. 5. Reflection coefficient through a protonated and unprotonated quinoid defect. The reflection coefficient vanishes at ~0.31β, indicating that the states at that energy are extended. [Reprinted from (36) with permission, © 1991 American Physical Society]
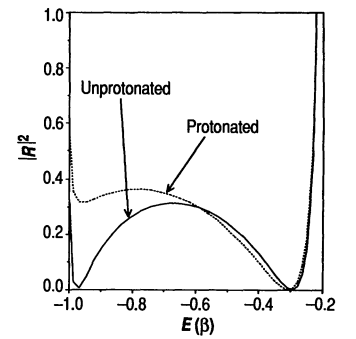
are assigned the site energy E_1 and are connected by the effective matrix element V_1. Our new lattice is equivalent to the RDM with the site energies E_1 appearing in pairs. All other nitrogens are assigned the renormalized bare energy $E_0 = \varepsilon_0 + 2t_2' \widetilde{V}_1$ and are connected by the matrix element V_0 (Fig. 4B). Protonation of the lattice simply changes the site energies E_1. Consequently, emeraldine and protonated emeraldine can be described by a RDM with off-diagonal disorder. Hence, in this version of the RDM, there are two kinds of dimer effects, protonated and unprotonated. As a consequence, it is not obvious that a set of unscattered electronic states exists.

We now show that this version of the RDM also exhibits a set of delocalized or conducting states. As we have done above, we simply compute the reflection and transmission coefficients through the protonated and unprotonated defect. We want to show that the reflection coefficient through both kinds of defects vanishes at an energy in the vicinity of the Fermi level. Consequently, the states at that energy are unscattered conducting states. We compute the reflection coefficient through a quinoid defect the way we did in the RDM. The result is given below:

$$|R|^2 = \frac{(V_1^2 - V_0^2 - W^2 - 2V_0 W \cos k)^2}{(V_1^2 - V_0^2 - W^2 - 2V_0 W \cos k)^2 + (2V_0 V_1 \sin k)^2} \tag{9}$$

Note that Eq. 9 reduces to Eq. 2 in the limit that $V_1 = V_0$. One can find a nontrivial solution for the vanishing of the reflection probability by numerically solving Eq. 1. We first calculated the energy band of leucoemeraldine. We chose the transfer matrix elements and site energies on the basis of optimized polyaniline geometries of Tanaka et al. (34) and in accordance with the molecular orbital calculations of Streitweisser (38) such that the experimentally observed band gap of 1.2β (18) was obtained. The term β is the resonance energy for benzene, which is ~2.5 eV. We then solved for the vanishing of Eq. 9 using the calculated energy band for leucoemeraldine. The reflection coefficient for a quinoid defect in the highest occupied leucoemeraldine band is shown in Fig. 5. Whether or not the quinoid defect is protonated, the reflection coefficient vanishes at ~ -0.31β (Fig. 5). Hence, the states at ~ -0.31β are completely unscattered by the quinoid defect and thus are conducting states. Because the reflection coefficient vanishes identically at -0.31β for a single defect, it will also vanish in a lattice containing an arbitrary concentration of randomly placed defects at this energy. The energy at which the reflection coefficient vanishes is independent of the concentration of defects (see above). Consequently, a randomly protonated emeraldine chain of arbitrary length should exhibit a set of conducting states in the vicinity of -0.31β. In the absence of any protonation, the Fermi level lies at -0.21β. The states at -0.21β are strongly localized because the reflection coefficient at that energy is unity (Fig. 5). Galvao et al. (19) showed that when the polymer is protonated the Fermi level moves contin-

uously from -0.21β to $\sim -0.35\beta$ at a protonation level of 50%. At this level the polymer exhibits its maximum conductivity. Hence, the energy of the current-carrying states in the RDM of protonated emeraldine is in agreement with the location of the extended states as calculated by Galvao *et al.* (*19*). More importantly, the energy of the current-carrying states in the RDM of protonated polyaniline is in close proximity to the location of the Fermi level when the polymer exhibits its maximum (50% protonated) conductivity. We argue that the metal-insulator transition in polyaniline is an instance of the RDM.

We now determine the width of the conducting states that we have shown to exist in single strands of polyaniline at zero temperature. We can obtain an estimate of the number of conducting states by expanding the reflection coefficient about the energy (E_0) at which Eq. 9 vanishes. To lowest order in $\Delta E = E - E_0$, we find that $|R|^2 \approx (\Delta E)^2$. From the arguments put forth in the previous section, we find that the total fraction of states whose mean free paths exceed the system size scales as $1\sqrt{N}$. Equivalently, $\sqrt{N}$ of the electronic states are unscattered by the disorder. Hence, in a single strand of the polymer, the width of the conducting states in the vicinity of E_0 is the square root of the length of the polymer chain. The length of the chains used by Galvao *et al.* (*19*) was 200. Hence, we estimate that the width of the conducting states is $\sim 0.06\beta$. Such a width of conducting states centered at -0.31β is certainly sufficient to explain the conducting states observed by Galvao *et al.* (*19*) and the conductivity maximum of polyaniline at a protonation level of 50%.

An immediate consequence of the model we have presented is that the conduction in each strand is metallic for doping levels in the vicinity of 50% at zero temperature. However, experimental measurements (*28*) of the conductivity at finite temperatures indicate that at all protonation levels the conductivity has the form $\sigma = \sigma_0 \exp[-(T_0/T)^{1/2}]$ where σ_0 and T_0 are temperature-independent constants. This behavior is more indicative of hopping conductivity than metallic transport. Experiments also indicate that T_0 is roughly a quadratic function of the protonation level in the protonation range of 20 to 50%. Three basic models give rise to a temperature dependence of the form $\exp[-T_0/T)^{1/2}]$ for the conductivity: (i) activated tunneling models for granular metals (*39*), (ii) 3-D variable-range hopping in the presence of a Coulomb gap (*40*), and (iii) 1-D variable-range hopping (*41*). Materials such as composites of nickel and SiO_2 form a granular structure containing grains of the metal separated by islands of the insulator SiO_2. Conduction obtains as a consequence of activated tunneling between the metallic grains. Sheng, Abeles, and Arie (*39*) showed that if the assumption is made that the product of the average separation between grains and the charging energy is constant, the desired temperature dependence of the conductivity is obtained. Recently Adkins (*42*) has shown that this assumption is not valid for several granular metals and in general is an ad hoc ansatz. He concluded that a satisfactory theory for electron transport in granular metals is lacking (*42*). Consequently, the applicability of the granular metal picture to amorphous systems such as polyaniline is certainly suspect. The Coulomb gap model of Efros and Shklovskii (*40*) is relevant to systems in which the density of states vanishes at the Fermi level. However, experiments on the Pauli susceptibility (*22*) in polyaniline indicate that the density of states does not vanish at the Fermi level.

The only model remaining that is consistent with the observed temperature dependence is that of variable-range hopping in a 1-D system. Kurkijarvi has pointed out, however, that along a single strand of infinite length, transport among a distribution of localized states will always be thermally activated (*43*). This result arises because it is impossible for a particle to circumvent an infinitely high barrier on a linear chain. This result is somewhat irrelevant because

the strands are of finite length in any physical system (*44*). Brenig *et al.* (*44*) showed that in a system consisting of noninteracting chains of finite length, averaging over the hops of varying length along each chain will give rise to the desired temperature dependence $\exp[-(T_0/T)^{1/2}]$. The immediate utility of this result (*44*) is not clear because interchain hopping ultimately facilitates transport from one end of the sample to the other. If hops to neighboring chains are included, the resultant transport process will follow the 3-D law $\sigma = \sigma_0 \exp[-(T_0/T)^{1/4}]$ if the number of chains to which any chain is connected is comparable to the length of a single chain (*41*). That is, the system will act as if it were 3-D. If the connections to adjacent chains are successively severed so that a single chain is connected to only a few chains (relative to the average chain length), the dynamics should cross over to the result of the 1-D variable range (*45*). Such a system with a finite number of transverse connections is a quasi–1-D system.

Yuval and later Thouless have shown that any system that is long enough will exhibit 1-D behavior (*46*). That is, any system that is finite in all directions except one will exhibit 1-D behavior. Consequently, the dynamics of any quasi–1-D system exhibiting hopping conduction should cross over to the activated limit as the chain length increases. The length L_∞ at which this state of affairs obtains defines the 1-D limit. Consequently, 1-D variable range hopping will be observed in a quasi–1-D system only when the average chain length L is such that $L_\perp \ll L \ll L_\infty$, where $L_\perp$ is the length scale in the transverse direction over which a single chain is connected.

This serious constraint on the applicability of the variable-range hopping model appears to have been overlooked in previous work (*33, 45*). For example, Wang *et al.* (*33*) and Nakhmedov, Prigodin, and Samukhin (*45*) assumed that if only nearest neighbor connections between chains were considered, the quasi–1-D variable-range result would follow. Such a system is, however, inherently 3-D. The latter authors have divided the resultant conductivity into transverse ($\sigma_\perp$) and longitudinal ($\sigma_\parallel$) components. Although the conductivity is generally anisotropic, this separation is problematic, primarily because the physical significance of $\sigma_\perp$ and $\sigma_\parallel$ is not immediate in the usual experimental situation in which leads are connected to both ends of the sample. The perpendicular component to the conductivity would have a definite physical meaning if a lead were applied to the tip of the first strand and to the end of the last strand of the lattice. Because the latter scenario is virtually impossible to construct experimentally, the immediate utility of the separation into $\sigma_\perp$ and $\sigma_\parallel$ is not clear. Nonetheless, phase segregation (*18*) of polyaniline into conducting and insulating domains suggests that the transverse hopping distance is short.

In applying the variable-range hopping picture to polyaniline, we simply need to determine the constant T_0. Recall that T_0 scales as the inverse of the localization length. For doping levels close to 50%, the states of interest are the extended states in the vicinity of the Fermi level. These states are responsible for the current within a chain and are also the relevant states when the electron hops from chain to chain. Consequently, the appropriate localization length scales as $1/(\Delta E)^2$. The energy difference can be expressed in terms of the protonation level as $\Delta E = c_0 - \alpha x$, where x is the concentration of protonated defects and c_0 and α are constants of proportionality. Experimentally, it is clear that T_0 has an approximately quadratic form in the protonation range of $x = 0.3$ to 0.5 (*18*). At this level of protonation, the scaling behavior we have shown here for the localization length should be valid. Hence, the behavior of T_0 as predicted by the RDM is consistent with the experimental data at moderate protonation levels. At lower protonation levels, the scaling behavior of the localization length we have derived is no longer valid (because ΔE is large), as evidenced by the deviation of the experimental data from a quadratic dependence at low levels of protona-

tion. There is some experimental evidence that the density of states at the Fermi level $[N(E_F)]$ is linearly proportional to the protonation level x. If this dependence is taken into consideration, we obtain that $T_0 \approx x$ because $T_0 \approx 1/[(\text{localization length})xN(E_F)]$. The available experimental data between $x = 0.3$ and 0.5, however, displays a more quadratic than linear dependence on x.

A consequence of this model is that as the parent polymer leucoemeraldine is successively oxidized, the conductivity should increase as the Fermi level is swept through the location in the band where the conducting states lie and subsequently decrease as the Fermi level moves further into the band. This behavior was recently observed in experiments by Ofer, Crooks, and Wrighton (27) as the electrochemical potential was continuously varied over a wide range. The finite window of high conductivity spanned 0.6 eV. Such a window is narrow compared with the band width (2.6 eV) and hence is consistent with the narrow band of conducting states in the RDM. Our model is also consistent with the observed decrease in the conductivity of randomly substituted polyaniline derivatives (33). It is straightforward to show that methyl group substitutions on the benzene or quinoid rings, for example, change the location of the unscattered states relative to the Fermi level. Hence, at a certain protonation level, the conducting states might not be accessible. The states at the Fermi level will then be localized and the conductivity should decrease.

The General Random Bipolaron Lattice: Application to Polyparaphenylene

There are a number of other polymers, such as polypyrolle, polythiophene, and polyparaphenylene that are in the same general class of conducting polymers as polyaniline (see above). All of these polymers lack a degenerate ground state, and bipolaron conduction appears to play a significant role in the observed metal-insulator transition (25, 26). We want to show now that any random bipolaron lattice can be mapped onto a version of the RDM. All random bipolaron lattices contain randomly placed pairs of correlated spins. The spins need not occur on neighboring lattice sites. In general, the several lattice sites can be separated. The bipolaron in polyparaphenylene is shown in Fig. 6A. There is some debate about the exact number of benzene rings the bipolaron spans (47). The
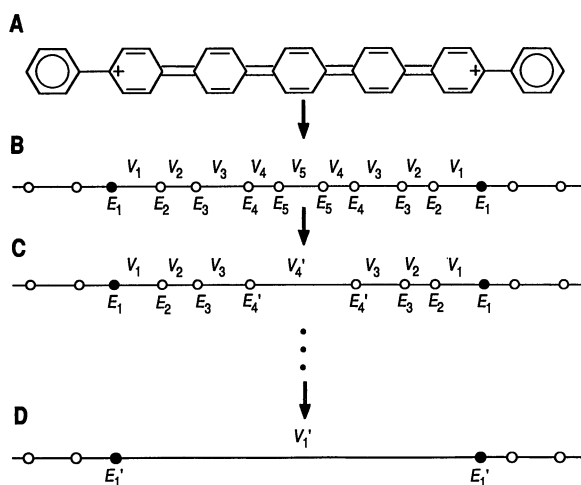
exact number is not crucial here. We want to show that regardless of the size of the bipolaron, it can be transformed into two adjacent lattice sites with equivalent energies. The same procedure used for polyaniline can be implemented here. First we reduce each benzene ring to two sites. The resultant lattice is shown in Fig. 6B. Regardless of the number of sites in each aromatic ring, the transformed ring will contain two sites. If the bipolaron ranges over M benzene rings, the reduced lattice will contain $2M + 1$ sites. The lattice sites 2 through $2M$ can all be decimated by systematically applying Kramer's rule to the eigenvalue equations for these sites. It is best to start this procedure at the middle of the bipolaron and decimate sites M and $M + 1$ first. After one application of Kramer's rule, the new site energies and matrix elements for sites $M - 1$ and $M + 1$ are

$$\Delta_i' = \Delta_i - V_i^2 \Delta_{i+1}/(\Delta_{i+1}^2 - V_{i+1}^2) \tag{10}$$

$$V_i' = V_i^2 V_{i+1}/(\Delta_{i+1}^2 - V_{i+1}^2) \tag{11}$$

where $\Delta_i = E - E_i$. After three subsequent transformations, the bipolaron reduces to the dimer shown in Fig. 6D. This procedure can be applied to any bipolaron lattice to reduce the bipolaron to two neighboring sites with new site energies and effective matrix elements connecting them. In general, any random bipolaron lattice can be mapped onto the RDM. This mapping raises the question of where the unscattered states lie relative to the Fermi level. By way of illustration, we computed the reflection coefficient through a bipolaron defect in polyparaphenylene. All parameters were chosen in accordance with those of Bredas et al. (47). Our preliminary results reveal that the reflection coefficient vanishes in the vicinity of the band edge, indicating the presence of conducting states at -0.62β. In the undoped form of the polymer, the Fermi level lies at -0.5β. Calculations are now under way to verify whether the Fermi level moves through the region of unscattered states as the polymer is doped. Should this behavior be observed, it is likely that the RDM will generally describe the metallic state in conducting polymers with nondegenerate ground states.

Repulsive Binary Alloy

Consider a binary alloy consisting of a- and b-type species. Assume the concentration of the b species is sufficiently small or that strong repulsions exist between b species such that along any axis of the alloy two b species do not appear in succession. We describe this alloy in the tight-binding approximation, in which the energy of the a- and b-type species is ε_a and ε_b, respectively. Let V_a and V_b be the nearest neighbor matrix elements connecting a-a and a-b sites, respectively. We have established that in one dimension, regardless of the concentration of the b-type defects (17), the repulsive binary alloy also exhibits an absence of localization whenever $V_a|\varepsilon_a - \varepsilon_b| \le 2|V_a^2 - V_b^2|$. Superdiffusive transport obtains when the strict inequality holds and diffusion when the equality is valid. Using arguments analogous to those used in the RDM, we find also that $\sqrt{N}$ of the electronic states are extended when this condition holds. The phases of the unscattered states in this model, however, do not change. The amplitude changes by the ratio V_a/V_b when an impurity is encountered. For example, if b-type impurities are located on sites -1 and 2, the unscattered eigenstate is $\cdots e^{-2ik}$, $(V_a/V_b) e^k$, 1, e^{ik}, $(V_a/V_b) e^{2ik}$, e^{3ik}, $\cdots$. The repulsive binary alloy applies to both the dilute limit of the binary alloy and physical systems such as Fibonacci lattices formed out of two kinds of materials. Let a = GaAs and b = AlAs. A Fibonacci sequence of a and b will be of the form a, ab, aba, abaab, . . ., where the nth entry is a product of the $(n - 1)$ and $(n - 2)$ entries. The b species appears

Fig. 6. (A) The bipolaron defect in polyparaphenylene. (B) The transformed lattice obtained by integrating out the benzene rings. Lattices (C) and (D) are obtained by a site decimation procedure that reduces the bipolaron to two neighboring sites with effective site energies and matrix elements.

singly; hence, a Fibonacci lattice is a subset of the repulsive binary alloy. Such semiconductor heterostructures have been fabricated experimentally because of the general interest in quasi-periodic order in crystals. The numerous theoretical treatments (48) of Fibonacci lattices have not predicted the transmission resonances we have discovered in the repulsive binary alloy because they have arranged either the matrix elements or the site energies in a Fibonacci sequence. As is evident from the repulsive binary alloy, the site energies in a Fibonacci lattice will follow the Fibonacci rule, but the matrix elements will not. These correlations have also been pointed out by Kumar (49) and elsewhere (50) in the context of Kronig-Penney models for Fibonacci lattices.

Final Remarks

We have considered a simple model in which the defects, by virtue of the pairing constraint, have internal structure. The internal structure leads to the resonance effect and the narrow band of conducting states when the defects are randomly placed. The analysis we have performed applies equally to trimers, quatramers, and so on. In fact, the reduction of the bipolaron in polyparaphenylene to a dimer-type defect demonstrates that any lattice containing randomly placed defects with internal structure can be reduced to the RDM. The only constraint on the internal structure is that it must contain a plane of symmetry, as in the case of bipolarons. As a new application, we have recently investigated the relevance of the RDM to the metallic state in heavily doped polyacetylene. It is straightforward to show that a neutral or charged soliton defect ranging over n sites in trans-polyacetylene can be reduced to a dimer defect—that is, solitons possess symmetric internal structure. Consequently, a single strand of polyacetylene containing a random distribution of solitons is equivalent to the RDM (51). It appears then that the RDM is of fundamental importance to the insulator-metal transition in conducting polymers both with and without degenerate ground states.

REFERENCES AND NOTES

1. P. W. Anderson, Phys. Rev. 109, 1492 (1958).
2. N. F. Mott and W. D. Twose, Adv. Phys. 10, 107 (1961).
3. R. Abou-Chacra, P. W. Anderson, D. J. Thouless, J. Phys. C 6, 1734 (1973).
4. R. E. Borland, Proc. R. Soc. London Ser. A. 274, 529 (1963).
5. H. Furstenberg, Trans. Am. Math. Soc. 108, 377 (1963).
6. H. Matsuda and K. Ishii, Prog. Theor. Phys. Suppl. 45, 56 (1968); K. Ishii, ibid. 53, 77 (1973); P. Dean and M. Bacon, Proc. R. Soc. London 81, 642 (1963).
7. For a review, see P. A. Lee and T. V. Ramakrishnan, Rev. Mod. Phys. 57, 287 (1985).
8. J. B. Pendry, J. Phys. C 20, 733 (1987).
9. F. Wegner, Z. Phys. B 25, 327 (1976). ·

10. E. Abrahams, P. W. Anderson, D. C. Licciardello, T. Ramakrishnan, Phys. Rev. Lett. 42, 673 (1979).
11. E. Cota, J. Jose, M. Ya. Azbel, Phys. Rev. B 32, 6157 (1985).
12. C. M. Soukoulis and E. N. Economou, ibid. 24, 5698 (1981).
13. T. F. Rosenbaum, K. Andres, G. A. Thomas, P. A. Lee, Phys. Rev. Lett. 46, 568 (1981).
14. D. J. Bishop, R. C. Dynes, B. Lin, D. C. Tsui, Phys. Rev. B 30, 3539 (1984).
15. G. A. Thomas et al., ibid. 24, 4886 (1981).
16. D. H. Dunlap, H.-L. Wu, P. Phillips, Phys. Rev. Lett. 65, 88 (1990).
17. H.-L. Wu and P. Phillips, J. Chem. Phys. 93, 7369 (1990).
18. R. de Surville, M. Josefowicz, L. T. Yu, J. Perichon, R. Buvet, Electrochim. Acta 13, 1451 (1968).
19. D. S. Galvao, D. A. dos Santos, B. Laks, C. P. de Melo, J. J. Caldas, Phys. Rev. Lett. 63, 786 (1989); ibid. 65, 527 (1990).
20. L. W. Shacklette, J. F. Wolf, S. Gould, R. H. Baughman, J. Chem. Phys. 88, 3955 (1988).
21. S. H. Glarum and J. H. Marshall, J. Electrochem. Soc. 134, 2160 (1987).
22. K. Mizoguchi, M. Nechtschein, J.-P. Travers, C. Menardo, Phys. Rev. Lett. 63, 66 (1989).
23. For a review see T.A. Skotheim, Ed., Handbook of Conducting Polymers (Dekker, New York, 1986).
24. W. P. Su, J. R. Schrieffer, A. J. Heeger, Phys. Rev. B 22, 2099 (1980).
25. J. Chen, A. J. Heeger, F. Wudl, Solid State Commun. 58, 251 (1986).
26. J.-L. Bredas and G. B. Street, Acc. Chem. Res. 18, 309 (1985).
27. D. Ofer, R. M. Crooks, M. S. Wrighton, J. Am. Chem. Soc. 112, 7869 (1990).
28. F. Zuo, M. Angelopuolos, A. G. MacDiarmid, A. J. Epstein, Phys. Rev. B 36, 3475 (1987); ibid. 39, 3570 (1989).
29. A. Litzelmann et al., Synth. Met. 29, 313 (1989).
30. W. R. Salaneck et al., ibid. 18, 291 (1987).
31. F. Wudl et al., J. Am. Chem. Soc. 109, 3677 (1987).
32. D. S. Boudreau et al., Chem. Phys. 85, 4584 (1986).
33. Z. H. Wang, E. Ehrenfreund, A. G. MacDiarmid, A. J. Epstein, Mol. Cryst. Liq. Cryst. 189, 263 (1990).
34. K. Tanaka, T. Shichiri, M. Kobashi, T. Yamabe, Synth. Met. 24, 167 (1988).
35. M. G. Kanatzidis, Chem. Eng. News 68, 36 (3 December 1990).
36. H.-L. Wu and P. Phillips, Phys. Rev. Lett. 66, 1366 (1991).
37. J.-L. Bredas, A. J. Epstein, A. G. MacDiarmid, ibid. 65, 526 (1990).
38. A. Streitweisser, Jr., Molecular Orbital Theory (Wiley, New York, 1961), p. 135.
39. P. Sheng, B. Abeles, Y. Arie, Phys. Rev. Lett. 31, 44 (1973).
40. A. L. Efros and B. I. Shklovskii, J. Phys. C. 8, L49 (1975).
41. N. F. Mott, Philos. Mag. 19, 835 (1969).
42. C. J. Adkins, J. Phys. C 20, 235 (1987).
43. J. Kurkijarvi, Phys. Rev. B 8, 922 (1973).
44. W. Brenig, G. H. Dohler, H. Heyszenau, Philos. Mag. 27, 1093 (1973).
45. E. P. Nakhmedov, V. N. Prigodin, A. N. Samukhin, Sov. Phys. JETP 31, 368 (1989).
46. G. Yuval, Phys. Lett. 53A, 136 (1975); D. J. Thouless, Phys. Rev. Lett. 39, 1167 (1977).
47. J.-L. Bredas, R. R. Chance, R. Silbey, Phys. Rev. B 26, 5843 (1982).
48. See, for example, M. Kohmoto, B. Sutherland, C. Tang, ibid. 35, 1020 (1987).
49. V. Kumar, J. Phys. Condens. Matter 2, 1349 (1990); see also G. Ananthakrishna, ibid., p. 1343.
50. J. Kollar and A. Suto, Phys. Lett. A 117, 203 (1986); F. Laruelle and B. Etienne, Phys. Rev. B 37, 4816 (1988).
51. In a forthcoming paper, we show that the extended states in the RDM for polyacetylene may account for the experimentally observed Pauli susceptibility that is independent of temperature in the heavily doped form of the polymer. The extension of the RDM to polyacetylene suggests that this model is of fundamental importance to the transport process in conducting polymers with and without degenerate ground states.
52. We thank D. H. Dunlap and P. E. Parris for their insights. Supported by NSF grant DMR8900303, the American Chemical Society Petroleum Research Fund, and the Whittaker College Health Sciences Fund.